VOLUME 8 (SPECIAL ISSUE) 2022

ISSN 2454-3055

Manuscripts under Special issue are published with the Theme
"Modern Perspectives of Biological Sciences"

Guest Editor: Dr. S. Mohanasundaram
Assistant Guest Editor: Dr. S.S. Syed Abuthahir

INTERNATIONAL JOURNAL OF ZOOLOGICAL INVESTIGATIONS

Forum for Biological and Environmental Sciences

Published by Saran Publications, India

International Journal of Zoological Investigations Vol. 8, Special Issue, 191-202 (2022)

International Journal of Zoological Investigations
Contents available at Journals Home Page: www.ijzi.net
Editor-in-Chief: Prof. Ajai Kumar Srivastav
Published by: Saran Publications, Gorakhpur, India

ISSN: 2454-3055

Identification of Potential Inhibitor Targeting InhA, Molecular Docking, ADMET, Molecular Dynamic Simulation and Antibacterial Activity of Thiazolidinone Derivatives: A Computational Approach

Jacquline Rosy P.[1*], Jebastin Sonia Jas M.[1], Santhanalakshmi K.[1], Venkat Kumar Shanmugam[2] and Prabhakaran A.[3]

[1]Department of Chemistry, IFET College of Engineering (Autonomous), Villupuram 605108, Tamil Nadu, India
[2]School of Biosciences and Technology, Vellore Institute of Technology, Vellore 632014, Tamil Nadu, India
[3]Department of Chemistry, CK College of Engineering and Technology, Cuddalore 607003, Tamil Nadu, India

**Corresponding Author*

Received: 14th August, 2022; **Accepted:** 25th September, 2022; **Published online:** 19th October, 2022

https://doi.org/10.33745/ijzi.2022.v08i0s.024

Abstract: This study was performed to examine molecular docking of newly synthesised thiazolidinone compounds and discover potential InhA inhibitors. MIC screening produced thiazolidinone derivatives for *Staphylococcus aureus* illness. KBr pellet FT-IR spectra were collected on a Thermo Nicolet AVATAR-330 spectrometer. Bruker obtained 400 MHz 1H spectra of all chemicals in DMSO-d6. Five 4-thiazolidinone derivatives:4-(4-oxo-2-phenylthiazolidin-3yl)amino)benzyl)oxazolidin-2-one(8), ((2-(4-chlorophenyl)-4oxothiazolidin-3yl)amino)benzyl)-oxazolidin-2-one(9), ((2-(4-fluorophenyl)-4-oxothiazolidin-3-yl)amino)benzyl)oxazolidin-2-one(10), 4-(4-((4-oxo-2-(p-tolyl)thiazolidin-3yl)amino)benzyl)oxazolidin-2-one(11) and 4-(4-((2-(4-methoxyphenyl)-4-oxothiazolidin-3yl)amino)benzyl)oxazolidin-2-one(12) docked due to its vast biological usefulness. Molecular docking, ADMET, TOPKAT Toxicity, and molecular dynamic simulation were used to estimate drug-likeness for 1QG6. MIC screening of synthesised thiazolidinone derivatives against *Staphylococcus aureus* through disc diffusion. Molecular docking studies examining the inhibitory effect of produced substances suggest testing for MIC antibacterial activity. Compound 12's antibacterial activity against *Staphylococcus aureus* is compared to Ampicillin and Cefixime. Compound 12 is utilised as an alternate medication for *Staphylococcus aureus*.

Keywords: Thiazolidinone derivatives, Inhibitors, *Staphylococcus aureus*, MIC screening, Molecular docking, Antibacterial activity

Citation: Jacquline Rosy P., Jebastin Sonia Jas M., Santhanalakshmi K., Venkat Kumar Shanmugam and Prabhakaran A.: Identification of potential inhibitor targeting InhA, molecular docking, ADMET, molecular dynamic simulation and antibacterial activity of thiazolidinone derivatives: A computational approach. Intern. J. Zool. Invest. 8(Special Issue):191-202, 2022.

https://doi.org/10.33745/ijzi.2022.v08i0s.024

Introduction

*Staphylococcus w*ithout treatment may be lethal as it infects body tissues. *Staphylococcus aureus* is a frequent human infection which causes gastroenteritis, meningitis, toxic shock syndrome, bacteremia, infective endocarditis, osteomyelitis, septic arthritis, lung infections, prosthetic device infections, and urinary tract infections. Treat *Staphylococcus* drug-resistant strains according to kind and presence. These bacteria might cause severe illnesses if they enter blood or tissues (Lowry, 1998). Intimate contact spreads certain illnesses (Rasigade and Vandenesch, 2014). *Staphylococcus aureus* genome has 22% non-coding (Fitzgerald *et al*., 2001).

Heterogeneity causes species diversity. Different strains promote antibiotic resistance or release different enzymes. *S. aureus* reproduces and evolves quickly, while AGR slows it down. Trading virulence for drug resistance has prolonged its genus. Sau1 Type I restriction-modification is another difficulty (RM). This digestion process protects the bacteria. The same enzymes allow DNA exchange across identical lines, but RM prevents line-to-line transfer (Lindsay, 2010).

Antibiotics cure *S. aureus* infections, and inappropriate antibiotic usage creates resistance. In 2005, MRSA fatalities equalled AIDS, TB, and viral hepatitis (Boucher *et al*., 2010). Computational modelling generates testable hypotheses. Network thinking is crucial for comprehending the multi-faceted consequences of medicine on a system, the adaptability of the system to therapy, and finding 'optimal approaches' rather than particular 'targets' for therapeutic intervention. Polypharmacology and combination targeting are popular (Chandra, 2010; Sivakumar *et al*., 2022). New ways to compute sRNA targets are being developed. Once targets are identified, regulatory RNA will be included in regulatory network models (Backofen and Hess, 2010).

Docking, molecular dynamics, QSAR modelling, PCA, and ADMET yielded the best results against SARS-CoV-2 (Islam *et al*., 2021). N-(4-nitrophenyl)-1H-tetrazol-5-amine is more active than thiourea on A549, HTB-140, and HaCaT cells. Results may assist to develop bioactive analogs (Bielenica *et al*., 2017). Survival requires enoyl acyl carrier protein reductases. These enzymes lengthen fatty acids. In bacteria, monofunctional proteins catalyse each process individually; in humans, a multifunctional protein does so.

Bacterial ENRs are good antibacterial medication targets since they do not change FAS I (Heath and Rock, 1995). In the final elongation step, acyl ENRs reduce enoyl-thioester (Bax *et al*., 2000). Many species share this fatty acid elongation step, although catalytic enzyme structure and organisation differ (Pearson, 2002). *S. aureus* reduces ENRs similarly. ENRs catalyse the last step of fatty acid elongation by reducing the C2-C3 carbon-carbon double bond generated by dehydratase enzymes (Rosy *et al*., 2017). This study was performed to examine molecular docking of newly synthesised thiazolidinone compounds and discover potential InhA inhibitors. MIC screening produced thiazolidinone derivatives for *Staphylococcus aureus* illness.

Materials and Methods

All solvents used were of spectral grade. All synthesised compounds' melting points were evaluated in open capillaries. FT-IR spectra were acquired on a Thermo Nicolet AVATAR-330 using KBr pellets. Bruker obtained 400 MHz 1H spectra of all chemicals in DMSO-d6. NMR spectra. For all NMR spectra, general procedure for preparation of (E)-4-(4-(2-arylindene hydrazinyl) benzyl) oxazolidin 2-one (3-7) & (E)-4-(4-((4-oxo-2-arylthiazolidin-3-yl) amino) benzyl) oxazolindin-2-one (8-12) is used.

Docking studies:

Five 4-thiazolidinone derivatives such as, 4-(4-oxo-2-phenylthiazolidin-3yl)amino)benzyl) oxazolidin-2-one (8), ((2-(4-chlorophenyl)-4 oxothiazolidin-3yl)-amino) benzyl) oxazolidin-2-one (9), ((2-(4-fluoro-phenyl)4-oxothiazolidin-3-yl)amino)

benzyl)oxa-zolidin-2-one (10),4-(4-((4-oxo-2-(p-tolyl)thiazo-lidin-3yl)amino)benzyl)-oxazolidin-2-one (11) and 4-(4-((2-(4-methoxyphenyl)-4-oxothiazolidin-3yl)amino)benzyl)oxazolidin-2-one (12) were docked.

Protein Data Bank provided 1QG6 reference proteins for our study (PDB). PyRx Version 0.8's AutoDock module was used for molecular docking. Blind docking and active site docking were used for ligand-receptor protein interactions. Blind docking was done on the 1QG6 PDB structure.

Chem-Draw Ultra 12.0 modelled ligand molecules for AutoDock 4.2, which Chem-Bio 3D Ultra 12.0 translated into 3D structures and saved as PDB. Next, AutoDock 4.2 was fed the produced ligands. A conventional docking strategy was employed for a stiff protein and ligand with torsion angles (for ten independent runs per ligand). The 0.375 grid and distance-dependent dielectric constant function were used to estimate the energetic map's x, y, and z coordinates. Other attributes are defaults.

ADMET:

The pharmacokinetic properties of the chosen ligands are critical for in vitro ADMET property prediction before taking the medication. Mol. 8, 9, 10, 11, and 12 ADMET properties were tested. This strategy can minimise time spent searching compound databases for possible lead chemicals with potential consequences. ADMET profile computation is key to prescription development and environmental risk management for pharmaceutical and chemical compounds. Discovery studio software models ADMET attributes to identify human adverse effects. The HIA model defines 95% and 99% confidence ellipses for ADMET AlogP98 aircraft (Balasubramaniyan *et al*., 2018; Ujjan *et al*., 2022).

TOPKAT analysis:

TOPKAT methodology tested Mol. 8, 9, 10, 11, and 12 for toxicity and degradation. TOPKAT estimated toxicological endpoints using QSTR models.

MDS:

For molecular dynamic modelling (MD), high-binding compounds in receptor 1QG6 were used. The MD molecule analyses 1QG6's temperature and stability. Standard dynamic cascade and minimization research protocol were utilised (Puratchikody *et al*., 2019).

Results and Discussion

Enoyl-acyl carrier protein reductase (*PDB code*: *1QG6*) *docking*:

RCSB PDB 1QG6 contains crystallographic enzyme ligand (Fig. 1). We docked all biologically active molecules to compare the binding affinity of newly synthesised thiazolidine analogues. Table 1 summarises dock stances' quantity and types. Docking experiments suggest that 8 and 10 have the same binding energy (-7.7 kcalmol^{-1}). Compound 8 established hydrogen bonds with ASN B: 175, TYR A: 104, ASN D: 257, and GLU D: 258. (Fig. 2 a-e). PRO A: 154 and LYS A: 205 interact alkyl-pi with molecule 8. Compounds 8 and 10 showed VdW and polar/electrostatic interactions. V148, D103, A100, F198, Y202, and G145 had VdW and polar/electrostatic interactions.

Fluoro substituent impact in compound 9 increases binding energy relative to the parent compound 8 and Ampicillin and Cefixime. Compound 11 has -7.8 kcalmol^{-1} binding energy. Compound 11's residues SER D, GLU B, and GLU A have VdW and polar/electrostatic interactions. Compound 12 has a good binding energy (-8.1 kcalmol^{-1}) with protein active site residues (Table 1), indicating that it can bind strongly to protein areas. It has four hydrogen bonds with TYR D:104, ASN A:257, LYS D:205, and ASN C:175. These proteins were docked into 1QG6, Ampicillin, and Cefixime to explain their lack of recognition at the enoyl-acyl carrier protein binding site.

ADMET:

Table 2 and Figure 3 show the ADMET analysis of Mol.8, 9, 10, 11 and 12. ADMET 2D PSA and AlogP confidence ellipses predict intestine absorption

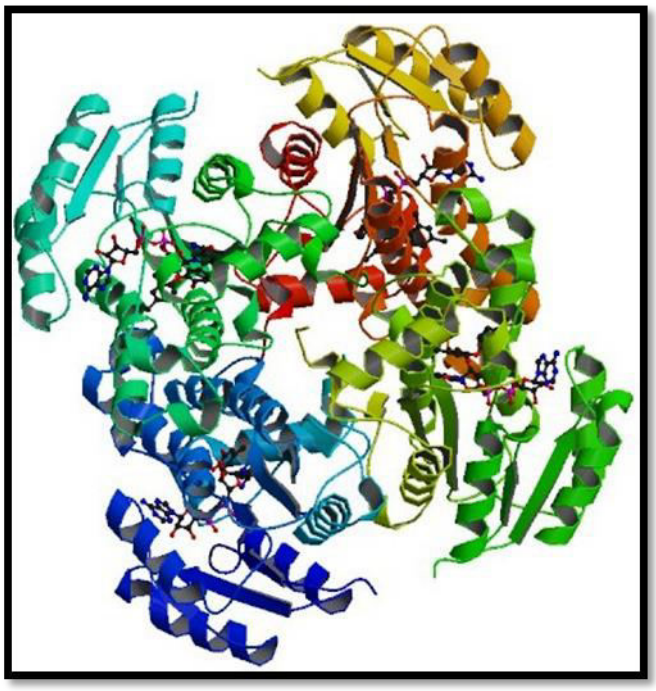

Fig. 1: 3D image of enoyl - acyl carrier protein reductase (PDB code: 1QG6).

Table 1: Docking results of the ligands 8 - 12 with enoyl acyl carrier protein reductase (PDB code: 1QG6)

Compounds	Substituent	Binding energy kcal.,mol^{-1}	Vdw_hb_desolv_ energy kcal.,mol^{-1}	Inhibition constant (µm)	Intermol energy kcal.,mol^{-1}	Hydrogen bonding	Residues involving interactions
8	H	-7.7	-6.21	504.46	-5.60	4	ASN B:175; TYR A:104; GLY A:102; PRO A:154; ASN D:257; GLU D:258; ASSP A:202; LYS A:205
9	F	-7.5	-7.04	64.343	-5.8	2	SER D:252; ARG B:171; GLU B:150; GLU A:150
10	Cl	-7.7	-5.68	56.20	-8.10	1	SER D:252; GLU B:150; GLU A:150
11	CH_3	-7.8	-6.37	54.96	-7.18	1	SER D:252; GLU B:150; GLU A:150
12	OCH_3	-8.1	-6.6	74.34	-7.12	4	TYR D:104; GLY D:102; PRO D:154; ASN A:257; ASP D:202; LYS D:205; ASN C:175
Co-ligand		-7.5	7.39	46.54	-6.56	-	LYS B:43; LEU B:44; LEU B:195; ALA B:15; TCL B:602;

							ALA B:196
Ampicillin		-6.8	-6.79	57.87	-7.4	5	GLU C:150; ARG B:151; VL D:244; GLU D:167; ARG D:171; ILE B:253; HIS B:246
Cefexime		-7.4	-8.4	60.56	-8.10	5	ARG C:171; GLU C:167; GLU D:157; AG B:151

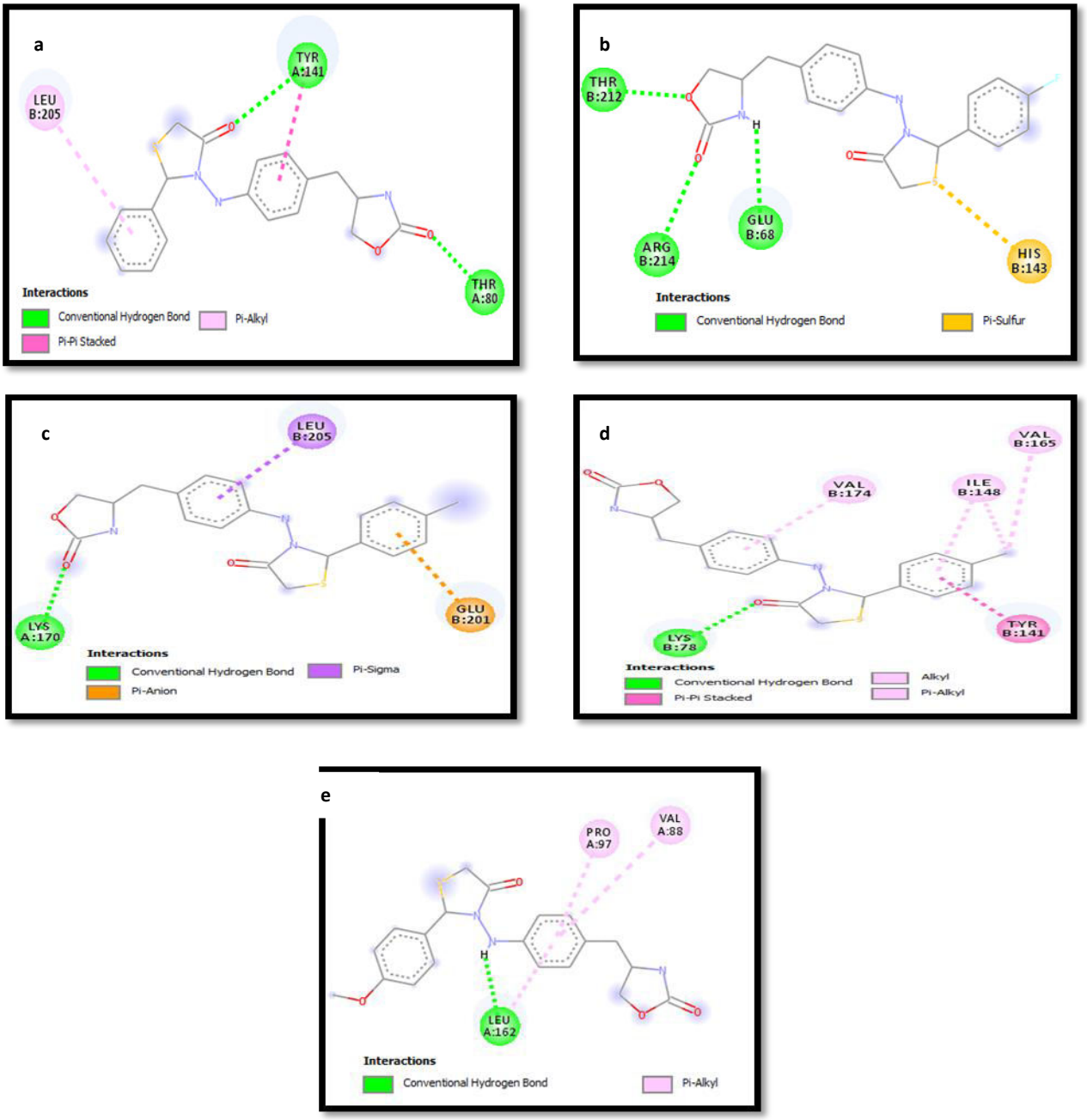

Fig. 2 (a-e): Docked conformation of most active compounds 8, 9, 10, 11 and 12 with hydrogen bonding in 2-D view.

Table 2: ADMET properties of the molecule M1, M2, M3 and M4

Mol. Name	Absorption level	Solubility level	BBB level	PPB level	Hepatotoxic level	CYP 2D6	PSA 2D	AlogP98
8	Good	Good	Low	<90%	No	No	77.21	3.26
9	Good	Good	Low	<90%	No	No	58.17	5.10
10	Good	Good	Low	<90%	No	No	69.14	4.95
11	Good	Good	Low	<90%	No	No	65.19	4.91
12	Good	Good	Low	<90%	No	No	52.37	3.52

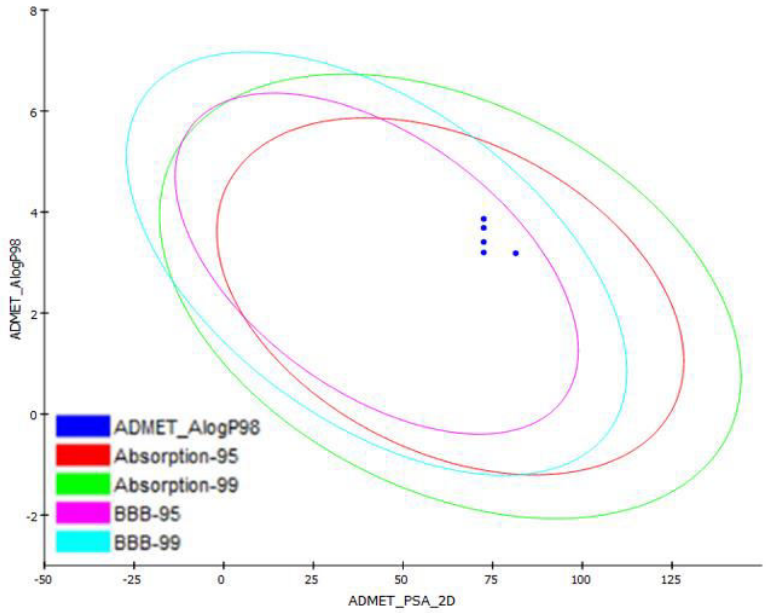

Fig. 3: Plot of polar surface area (PSA) versus ALogP for Mo.8, 9, 10, 11 and 12 showing the 95% and 99% confidence limit ellipses corresponding to the blood brain barrier (BBB) and intestinal absorption.

and blood-brain barrier penetration. The ellipses indicated where chemicals are well-absorbed. All molecules absorbed well (HIA). ADMET 95% and 99% confidence ellipses described HIA absorption levels.

All chemicals were aqueous-soluble. All compounds were adequate for CYP2D6 liver, suggesting PA are non-CYP2D6 inhibitors. The model orders "toxic" or "nontoxic" and gives a certainty level for the model's accuracy. All chemicals are harmless to the liver; therefore they undergo first-pass metabolism. According to the model, all compounds should have PSA 140 2 and AlogP98 5 for optimal cell permeability. All compounds had PSA140 2. All compounds had AlogP98 values 5. All compounds contain drug-like characteristics, according to ADMET.

A computational technique was used to determine the structural basis and selectivity mechanism of 3-substituted benzamide analogues as FtsZ inhibitors (Tripathy *et al*., 2018). 3D-QSAR and structure-based techniques were used to test compounds against ZINC database based on FtsZ inhibitors and crystal structure (Qiu *et al*., 2019).

TOPKAT (*Toxicity risk assessment*):

TOPKAT established a system to evaluate applicability using optimum predictive space (OPS). A chemical is within, outside, or borderline OPS. If the chemical is OPS, predictions should be accurate. Therefore, the borderline position was out of AD. In addition, fragments not in the training set can lead to incorrect estimates. Table 3 shows TOPKAT toxicity predictions. Animal models predicted the medication and chemical toxicity profiles. By analysing the probabilities, it can be inferred that Mol 8, 9, 10, 11, and 12 do not

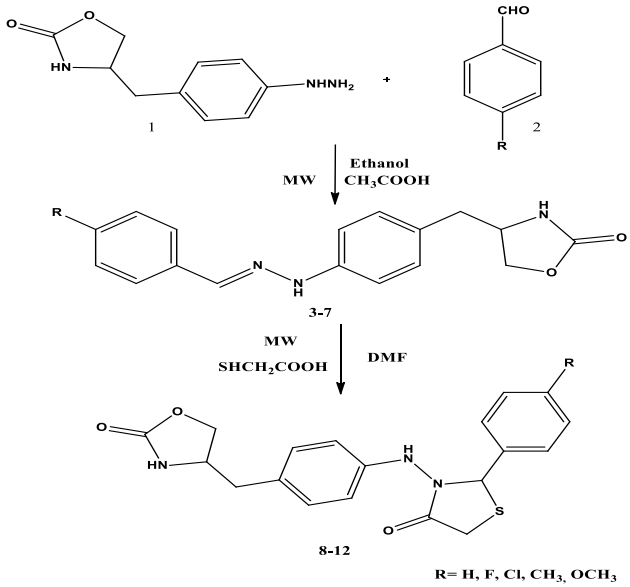

Fig. 4: Synthetic routes of compounds thiazolidinones.

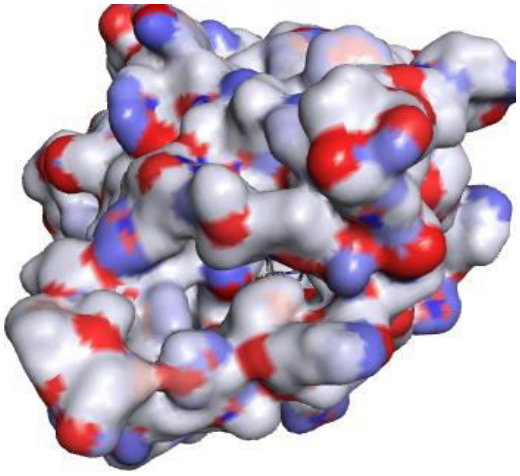

Fig. 5: The receptor 1QG6 with potent Mol. 12 compound.

diverge much and exhibit higher probabilities for NTP Carcinogenicity Call (Male Rat), Ames Mutagenicity, and NTP Carcinogenicity Call (Female Rat), while FDA Carcinogenicity Female Rat Non versus Carc is low. All compounds have the same FDA Carcinogenicity, Male Rat- Non against Carc, Ocular Irritancy MLD versus NON, and Aerobic Biodegradability profiles.

Molecular dynamics:

This MD simulation focuses on the receiver, drug-receptor-complex, temperature (K) mode conformation changes, and energy function. (Kcal/mol). According to the investigations, Mol. 12 is effective at molecular docking, ADMET, and toxicity prediction. So, MD was used to evaluate Mol. 8 with receptor 1QG6 (Fig. 4). We chose this complicated protein for MD stability studies. RMSD and RMSF were regulated during simulations to check 1QG6's stability with Mol.12 complex (RMSF). Figure 5 exhibits 1QG6 with Mol. 12 RMSD of 0.75. RMSD and RMSF analysis (Fig. 6)

Table 3: Predicted toxicity of the compounds

Model	Mol. 8	Mol. 9	Mol. 10	Mol. 11	Mol. 12
Ames Mutagenicity	No	No	No	No	No
NTP Carcinogenicity Call (Male Rat)	No	No	No	No	No
NTP Carcinogenicity Call (Female Rat)	No	No	No	No	No
NTP Carcinogenicity Call (Male Mouse)	No	No	No	No	No
NTP Carcinogenicity Call (Female Mouse)	No	No	No	No	No
Developmental Toxicity Potential	Non Toxic	Non Toxic	Non Toxic	Non Toxic	Non Toxic
Rat Oral LD_{50}	4.5	2.8	4.1	2.8	4.8
Rat Maximum Tolerated Dose – Feed/Water (v6.1) (mg/kg)	102.3	88.27	94.28	67.47	94.10
Rat Inhalational LC_{50} (v6.1) (g/m3/H)	4.3	4.7	4.1	4.1	4.9
Skin Irritation	No	No	No	No	No
Skin Sensitization	No	No	No	No	No
Ocular Irritancy	No	No	No	No	No
Aerobic Biodegradability	Biodegradable	Biodegradable	Biodegradable	Biodegradable	Biodegradable
Fathead Minnow LC_{50} µg/l)	3.0	5.7	7.1	6.2	8.1
Daphnia EC_{50} (mg/l)	56.4	48.4	51.1	68.1	58.2

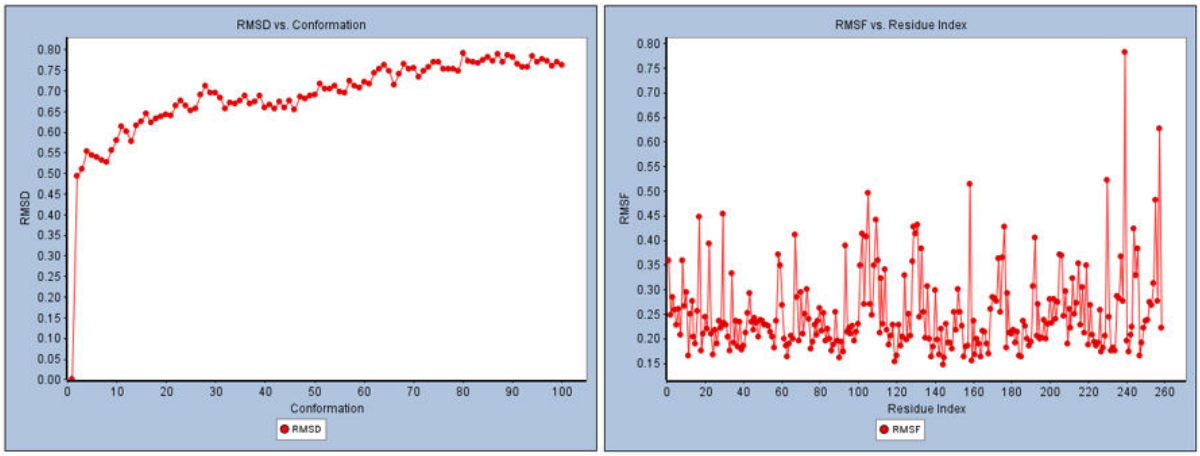

Fig.6: RMSF and RMSD of various confirmation of 1QG6 with potent Mol. 12 complex

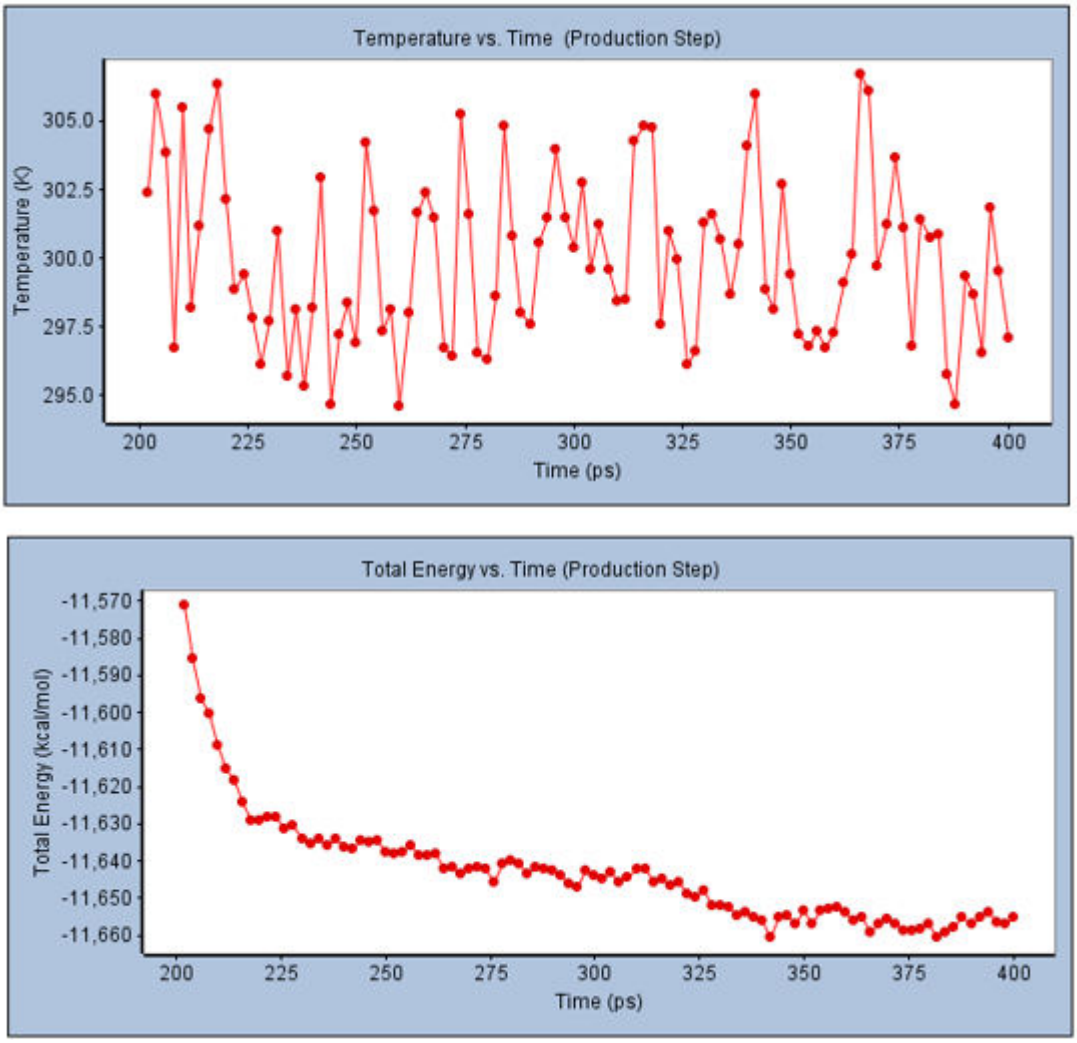

Fig. 7: Time based total energy and b) temperature changes in different time scale of 1QG6 with Mol.12 complex.

shows that the Mol. 12 complex ligand does not change 1QG6 structure or residue conformation. Figure 7 shows the energy difference and protein complex stabilisation temperature. At 400 ps from 295 to 305 K, Mol.12 receptors were stabilised at -11,650 Kcal/mol-. The MD results showed that Mol.12 does not impact the 1QG6 receptor's stability and structure.

Quantum mechanics/molecular mechanical study demonstrated non-binding interactions surrounding the complex interfaces of newly found antibacterials with GyrB ATPase and tyrosyl-tRNA synthetase as their targets and suggested a novel strategy to resist multifreeze anti-military chemicals. Zang *et al*. (2016) observed functionally characterised sRNAs. Receptor-based 3 D-QSAR and docking studies were utilised to explore molecule-receptor binding interactions that change inhibitory activity (Ballu *et al*., 2018).

Structure Activity Relationship-SAR:

Figure 8 shows the SAR deduced from AutoDock data. Our developed compounds are more active than the Co-ligand in 1QG6, Ampicillin, and Cefixime. Molecular docking studies evaluating the inhibitory effect of produced compounds suggested additional testing for MIC antibacterial activity.

MIC screening of antibacterial activity of synthesised thiazolidinone derivatives against *Staphylococcus aureus* through disc diffusion technique. Parallel tests determined ampicillin and cefixime MICs to measure organism

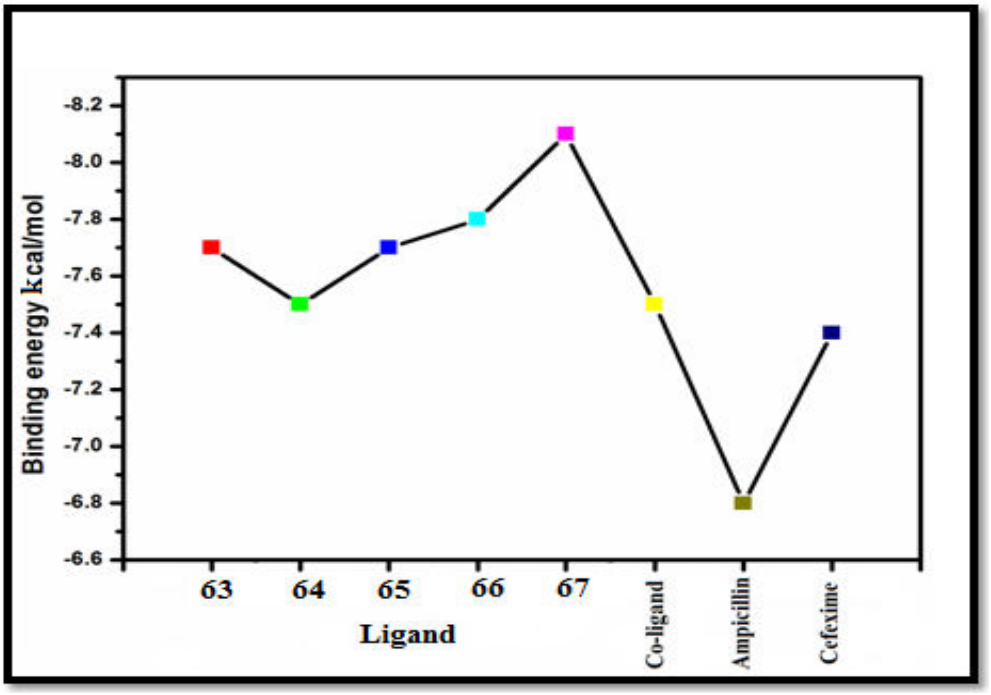

Fig. 8. In-silico activity of the tested compounds.

Table 4: Antibacterial activity (MIC) of compound 12 against the bacteria Staphylococcus aureus

Compound	**Concentration µg / ml**	**Zone of inhibition (mm/diameter)**
		Staphylococcus aureus
Control	-	-
Ampicillin	100	24
Cefexime	100	16
12	50	14
	100	16
	150	18

sensitivity. Table 4 compares compound 12's antibacterial efficacy against *Staphylococcus aureus* to Ampicillin and Cefixime. Control DMSO revealed no inhibitory zone. Mol. 12 is most active against *Staphylococcus aureus* with a Minimal Inhibitory Concentration (MIC) of 150 µg/ml (18 mm) and minimum activity at 50 µg/ml (14 mm). Cefixime showed virtually the same inhibition at100 g/ml as compound 12, whereas Ampicillin showed stronger inhibition. Compound 12 is a good alternative medication for *Staphylococcus aureus* (Fig. 9). The present-day focus is on emerging tools to correctly calculating sRNA targets and once targets are known, the next task

Fig. 9: Antibacterial activity (MIC) of compound 12 against the bacteria *Staphylococcus auereus.*

will be the popular integration of regulatory RNA in the prevailing models of regulatory networks. (Backofen and Hess, 2010).

Docking, molecular dynamics, QSAR modelling, PCA, and ADMET have produced the finest pictures against SARS-protease CoV-2's (Islam *et al*., 2021). N-(4-nitrophenyl)-1H-tetrazol-5-amine was shown to be more active than thiourea on A549, HTB-140, and HaCaT cell lines using MTT test. Results may help create a new family of bioactive analogs (Bielenica *et al*., 2017).

Conclusion

4-thiazolidinone derivatives were docked against enoyl acyl carrier protein reductase (1QG6) using PyRx'sAutoDock module. Most produced compounds (8-12) had good inhibition and binding affinity. Synthesized compounds have binding scores between -7.1 and -8.8. Compounds 8, 11 and 12 have the most receptor-protein binding energy. Good Glide ratings are attributed to compounds' lipophilicity and hydrogen bonding. According to these investigations, 4-thiazolidinone compounds are gaining popularity for their antibacterial capabilities. Considering the importance of 4-thiazolidinone in antibacterial activities, some novel 4-thiazolidinone were created utilising AutoDock molecular modelling software. ADMET and TOPKAT toxicity studies demonstrate compounds which have drug-like characteristics and no harmful fragments. Designed compounds with better in-silico activity were studied for MIC. The compounds are synthesized by microwaves. Microwave approach offered good results in less time than conventional., The compounds studied in this study exhibited good antibacterial activity against diverse strains. Synthesized derivatives showed that 4-thiazolidinone rings are pharmacologically active backbones. The pharmacological evaluation of tested compounds has revealed promising results, which may lead to the identification of powerful antibacterial drugs.

References

Backofen R and Hess WR. (2010) Computational prediction of sRNAs and their targets in bacteria. RNA Biol. 7(1): 33-42.

Balasubramaniyan S, Irfan N, Umamaheswari A and Puratchikody A. (2018) Design and virtual screening of novel fluoroquinolone analogs as effective mutant DNA GyrA inhibitors against urinary tract infection-causing fluoroquinolone resistant *Escherichia coli*. RSC Adv. 8(42): 23629-23647.

Ballu S, Itteboina R, Sivan SK and Manga V. (2018) Structural insights of *Staphylococcus aureus* FtsZ inhibitors through molecular docking, 3D-QSAR and molecular dynamics simulations. J Recept Signal Transduct. 38(1): 61-70.

Bax R, Mullan N and Verhoef J. (2000) The millennium bugs--the need for and development of new antibacterials. Int J Antimicrob Agents 16(1): 51-59.

Bielenica A, Szulczyk D, Olejarz W, Madeddu S, Giliberti G, Materek IB and Koziol AE. (2017) Struga M. 1H-Tetrazol-5-amine and 1,3-thiazolidin-4-one derivatives containing 3-(trifluoromethyl)phenyl scaffold: Synthesis, cytotoxic and anti-HIV studies. Biomed Pharmacother. 94: 804-812.

Boucher H, Miller LG and Razonable RR. (2010) Serious infections caused by methicillin-resistant *Staphylococcus aureus*. Clin Infect Dis. 51 (Suppl 2): S183-S197.

Chandra N. (2009) Computational systems approach for drug target discovery. Expert Opin Drug Discov. 4(12): 1221-1236.

Fitzgerald JR. (2014) Evolution of *Staphylococcus aureus* during human colonization and infection. Infect Genet Evol. 21: 542-547.

Fitzgerald ML, Mendez AJ, Moore KJ, Andersson LP, Panjeton HA and Freeman MW. (2001) ATP-binding cassette transporter A1 contains an NH2-terminal signal anchor sequence that translocates the protein's first hydrophilic domain to the exoplasmic space. J Biol Chem. 276(18): 15137-15145.

Heath RJ and Rock CO. (1995) Enoyl-acyl carrier protein reductase (fabI) plays a determinant role in completing cycles of fatty acid elongation in Escherichia coli. J Biol Chem. 270(44):26538-26542.

Islam R, Parves MR, Paul AS, Uddin N, Rahman MS, Mamun AA, Hossain MN, Ali MA and Halim MA. (2021) A molecular modeling approach to identify effective antiviral phytochemicals against the main protease of SARS-CoV-2. J Biomol Struct Dyn. 39(9): 3213-3224.

Lindsay JA. (2010) Genomic variation and evolution of *Staphylococcus aureus*. Int J Med Microbiol. 300(2-3): 98-103.

Lowry FD. (1998) *Staphylococcus aureus* infections. N Engl J Med. 339(8): 520-532.

Pearson H. (2002) Superbug hurdles key drug barrier. Nature 418(6897): 469.

Puratchikody A, Irfan N and Balasubramaniyan S. (2019) Conceptual design of hybrid PCSK9 lead inhibitors against coronary artery disease. Biocatalysis Agricult Biotechnol. 17: 427-440.

Qiu Y, Zhou L, Hu Y and Bao Y. (2019) Discovery of promising FtsZ inhibitors by E-pharmacophore, 3D-QSAR, molecular docking study, and molecular dynamics simulation. J Recept Signal Transduct Res. 39(2): 154-166.

Rasigade JP and Vandenesch F. (2014) *Staphylococcus aureus*: a pathogen with still unresolved issues. Infect Genet Evol. 21: 510-514.

Rosy PJ, Kalyanasundaram S, Santhanalakshmi S and Muthukumar K. (2017) Microwave Synthesis, spectroscopic characterization and DFT investigation of 4-(4-(2-(4-substitutedphenyl)-4-oxothiazolidin-3-yl) benzyl) oxazolidin-2-one derivatives. World Scientific News 69: 122-142.

Sivakumar S, Mohanasundaram S, Rangarajan N, Sampath V and Dass Prakash MV. (2022) In silico prediction of interactions and molecular dynamics simulation analysis of Mpro of Severe Acute Respiratory Syndrome caused by novel coronavirus 2 with the FDA-approved nonprotein antiviral drugs. J Appl Pharm Sci. 12(05): 104-119.

Tripathy S, Azam MA, Jupudi S and Sahu SK. (2018) Pharmacophore generation, atom-based 3d-qsar, molecular docking and molecular dynamics simulation studies on benzamide analogues as ftsz inhibitors. J Biomol Struct Dyn. 36(12): 3218-3230.

Ujjan JA, Morani W, Memon N, Mohanasundaram S, Nuhmani S and Singh BK. (2022) Force platform-based intervention program for individuals suffering with neurodegenerative diseases like Parkinson. Comput Math Methods Med. 2022: 1636263.

Zang P, Gong A, Zhang P and Yu J. (2016) Targeting druggable enzymome by exploiting natural medicines: An *in silico-in vitro* integrated approach to combating multidrug resistance in bacterial infection. Pharm Biol. 54(4): 604-618.